EFFICIENT PATH KERNELS FOR REACTION FUNCTION PREDICTION

Markus Heinonen*, Niko Välimäki*, Veli Mäkinen and Juho Rousu
Department of Computer Science, University of Helsinki, Helsinki, Finland
{*mqheinon, nvalimak, vmakinen, rousu*}*@cs.helsinki.fi*

Keywords: Graph kernels, Compressed data structures, XBW transform, Reaction graph, Hierarchical classification.

Abstract: Kernels for structured data are rapidly becoming an essential part of the machine learning toolbox. Graph kernels provide similarity measures for complex relational objects, such as molecules and enzymes. Graph kernels based on walks are popular due their fast computation but their predictive performance is often not satisfactory, while kernels based on subgraphs suffer from high computational cost and are limited to small substructures. Kernels based on paths offer a promising middle ground between these two extremes. However, the computation of path kernels has so far been assumed computationally too challenging. In this paper we introduce an effective method for computing path based kernels; we employ a Burrows-Wheeler transform based compressed path index for fast and space-efficient enumeration of paths. Unlike many kernel algorithms the index representation retains fast access to individual features. In our experiments with chemical reaction graphs, path based kernels surpass state-of-the-art graph kernels in prediction accuracy.

1 INTRODUCTION

Kernel methods have proven an efficient approach in machine learning tasks, such as classification, regression and clustering (Shawe-Taylor and Christianini, 2004). A kernel defines a similarity function between two objects, which corresponds to implicitly mapping the objects to a feature space, in which a dot product equals the kernel value. This property of kernels is especially suitable for complex structural data, as the object's vectorial representation is formed automatically.

Graph kernels try to capture the essential topological features of the graph by providing a (possibly infinite) feature vector representation of the graph, and subsequently computing the similarity between the feature vectors. Paired with kernel methods, the relevant application-dependent substructure signals can be exploited. Graph kernels can be categorised based on the generality of the feature class: sequence based kernels enumerate e.g. walks or paths, subtree based kernels allow sequences to branch, and subgraph based kernels place no restrictions on the substructure.

The commonly used walk kernels can be computed efficiently up to infinite length, but they contain arbitrary repeats of themselves (Gärtner, 2003). Any walk can continue infinitely by traversing itself back and forth. These repeated walks contain no additional information about the graph, however they result in infinite feature space and in kernels with large norms. Down weighting longer walks alleviates the problem (Gärtner, 2003). In (Mahe et al., 2005) the problem was fought by introducing non-tottering walks, where tottering cycles of length two are prohibited in walks.

Kernels based on paths, that is walks with no repetitions, are more challenging to compute and few practical algorithms so far exists. In (Borgwardt et al., 2005) an efficient kernel using shortest paths between nodes in the graphs was proposed. The shortest paths kernel has an exceptionally small feature space as there only exists n^2 shortest paths in a graph of size n, which makes its efficient to compute. In (Ralaivola et al., 2005) a suffix trees was utilized in computing the pairwise path kernels individually up to length 10. However, so far a method for efficiently computing an all-paths kernel has been missing. In this paper we propose an efficient method for computing path kernels using a compressed path index as an intermediate data structure. The compressed path index is based on a Burrows-Wheeler transform of labeled trees (Ferragina et al., 2009) and contains the feature values explicitly which allows for various kernel functions in the feature space.

*Equal contribution from these authors

We take two steps to compute path kernels when given a set of graphs as an input: First, we create a specialized *path index* that represents all the paths, up to some maximum length, of all graphs in compressed form and allows us to efficiently traverse all unique paths and output their frequencies for desired graphs. Then, the path frequencies are used to compute path kernels via inner products. In our experiments we compare path based graph kernels against walk based kernels, shortest paths based kernels, as well as the custom reaction graph kernel by (Saigo et al., 2010). The performance is evaluated in a hierachical multilabel classification task of assigning a biochemical reaction to the correct branch of the Enzyme Commision (EC) hierarchy.

In section 2 we review existing sequence based kernels on graphs, including the shortest paths kernel. In section 3 the compressed path index for the computation of path kernels is introduced. In section 4 experiments are carried out where the path based kernels are compared against state-of-the-art graph kernels. We also review the run time performance of our method. We conclude with discussions in section 5.

2 GRAPH KERNELS

In this section we review existing approaches for computing graph kernels. We consider a labeled undirected graph $G = (V, E, L)$ with n nodes, where a labeling function L applies to both nodes $v \in V$ and edges $(v,u) \in E$. A *walk* w is a sequence of adjacent vertices. A path p is a walk where no node repeats.

Random walk kernels compute the weighted sum of matching walks in a pair of graphs, utilizing either the adjacency matrix exponential (Gärtner, 2003) or a markov process model (Kashima et al., 2003). If the contribution of each walk is downscaled appropriately according to its length k with λ^k the walk kernel can be computed until convergence in cubic time. An generalization to marginalized kernels prevents nontottering walks by utilizing second order markov processes (Mahe et al., 2005).

With $\lambda < 1$ the contribution of longer walks quickly becomes negligible and long walks have effectively no effect on the kernel value in the standard walk kernel. This is sometimes against what we desire – longer walks may contain important information for e.g. graphs with repetitive substructures, where the walk length is required to surpass the diameter of the substructure to notice the repetition. Therefore we consider finite-length walk kernels, where walks up to length k are constructed explicitly. Working with explicit walks allows us to regard paths and non-tottering walks. We can count the number of matching k-length walks in two graphs by using dynamic programming (Demco, 2009).

Borgwardt et al. defined a family of kernels using special subsets of paths, namely the set of shortest paths between all nodes (Borgwardt et al., 2005). All pair shortest paths can be computed with Floyd-Warshall algorithm in $O(n^3)$ time. The kernel is then defined $K_{sp}(G,G') = \sum_{p \in \mathcal{SP}(G), p' \in \mathcal{SP}(G')} K_l(p,p')$, where $\mathcal{SP}(G)$ is the set of shortest paths between all nodes of graph G and K_l is a positive semi-definite path matching kernel. However, in many applications it is not clear that shortest paths carry a special meaning. Thus efficient methods to compute path kernels with a broader feature space is still desirable.

3 COMPUTING PATH KERNELS VIA COMPRESSED PATH INDEX

We wish to use the set of all paths to characterize a given graph. We define an all paths kernel as a dot product between shared path counts. Computing the path kernel is known to be NP-hard (Borgwardt et al., 2005). However, we will show here that it is possible to compute them with typical molecular datasets such as KEGG reaction database.

We use a four-fold procedure to compute the kernel. First, trees up to height h of all graphs are enumerated using each node subsequently as the root node. Then, the resulting trees are used as an input to a path index construction. Finally, the feature values are extracted from the index, and the kernel is explicitly computed.

Path Enumeration. For each vertex $u \in V$, we build a tree T_u that contains all paths originating from u. This can be done with a depth-first traversal in G, and the result is a set of trees $\mathcal{T} = \{T_u \mid u \in V\}$. Figure 1 gives an example of a graph and one of the trees generated. When multiple graphs $G_1, G_2, \ldots, G_g$ are given, each graph can be processed separately creating a set of tree sets $\mathcal{T}_1, \mathcal{T}_2, \ldots, \mathcal{T}_g$. Path enumeration can be generalized to *directed* and *edge-labeled* graphs.

Path Index Construction. We store the set of trees as a path-sorted transform dubbed XBWT (Ferragina et al., 2009). We will show how the resulting index can be used to efficiently compute path frequencies,

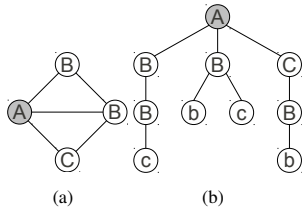

S_{last}	S_α	S_π
0	A	*empty*
0	B	A
0	B	A
1	C	A
1	B	BA
0	b	BA
1	c	BA
1	c	BBA
1	b	BCA
1	B	CA

(c)

Figure 1: (a) Example graph. (b) Paths originating from node A. (c) An XBWT representation of the tree in (b). The rows are lexicographically sorted by upward paths, S_π, which are displayed here for reference and not stored at any point of the algorithm.

but first, let us describe how to construct the transform for a single tree T of t nodes.

The XBWT of T is constructed in two phases (Ferragina et al., 2009). The first phase starts by initializing an array $S[1,t]$ to contain the nodes in pre-order: for each node u, we store its label $\alpha[u]$, a parent pointer and a boolean value $\mathsf{last}[u]$. We set $\mathsf{last}[u] = 1$ if u is the right-most child of its parent. Finally, we need to be able to distinguish between internal and leaf node labels — for example, in Figure 1, we use lower-case labels for leaves. In the second phase, S is stably sorted according to the lexicographical order of node's *upward path* $\pi[u]$, that is, the labeled path from u to the root. In (Ferragina et al., 2009) an optimal $O(t)$-time algorithm was given to sort S in *implicit* manner, without a need to store the $\pi[u]$ values explicitly.

The final XBWT of T consists of a bitvector S_{last} and an array of node labels, denoted by S_α. They are populated simply by following the order the nodes appear in S after the sorting phase. Figure 1(c) gives an example of values of S_α and S_{last} for the tree in Figure 1(b). The actual index, which grants us navigational operations on T and efficient way of counting path frequencies, requires rank and select queries on S_α and S_{last}. The query $\mathsf{rank}_c(S_\alpha, i)$ gives the number of times c appears in $S_\alpha[1,i]$, and $\mathsf{select}_c(S_\alpha, i)$ gives the position of the i-th c in S_α. Both of these queries can be solved in $O(\log\sigma/\log\log t)$ time, for any alphabet size $\sigma = O(t^\varepsilon)$ and $\varepsilon < 1$, by using a *Wavelet tree* data structure requiring $tH_0(S_\alpha) + o(t\log\sigma)$ bits of memory (Ferragina et al., 2007), where $H_0(S_\alpha) \leq \log\sigma$ is the 0-th order entropy of S_α Thus, the whole index requires in total $tH_0(S_\alpha)+t+o(t)$ bits, plus another t bits if we use an additional bitvector to distinguish leaf node labels. The XBWT representation

Algorithm $\mathsf{traverse}(s, e, P, lf)$:
1 $C \leftarrow$ Set of internal node symbols on $S_\alpha[s,e]$.
2 $L \leftarrow$ Set of leaf node symbols appearing on $S_\alpha[s,e]$.
3 **for each** $c \in C$ **do**
4 $\quad lf' \leftarrow 0$
5 $\quad$ **if** $\mathsf{leaf}(c) \in L$ **then**
6 $\quad\quad L \leftarrow L \setminus \mathsf{leaf}(c)$
7 $\quad\quad lf' \leftarrow$ Number of $\mathsf{leaf}(c)$ in $S_\alpha[s,e]$.
8 $\quad z_1 \leftarrow \mathsf{select}_c(S_\alpha, \mathsf{rank}_c(S_\alpha, s-1)+1)$
9 $\quad z_2 \leftarrow \mathsf{select}_c(S_\alpha, \mathsf{rank}_c(S_\alpha, e))$
10 $\quad s' \leftarrow \mathsf{GetRankedChild}(z_1, 1)$
11 $\quad e' \leftarrow \mathsf{GetRankedChild}(z_2, \mathsf{GetDegree}(z_2))$
12 $\quad \mathsf{traverse}(s', e', cP, lf')$
13 **for each** $c \in L$ **do**
14 $\quad lf' \leftarrow$ Number of leaf symbols c in $S_\alpha[s,e]$.
15 $\quad$ Output subpath cP with frequency lf'.
16 $f \leftarrow \mathsf{rank}_1(S_{\text{last}}, e) - \mathsf{rank}_1(S_{\text{last}}, s-1)$
17 Output subpath P with frequency $f + lf$.

Figure 2: Recursive algorithm to traverse through all uniquely labeled, root-originating paths. The first call of the recursion is $\mathsf{traverse}(1, 1, \mathit{empty}, 0)$. Function $\mathsf{leaf}(c)$ is just a simple conversion between internal and leaf node labels, e.g. an upper-case conversion in Figure 1.

generalizes to multiple trees quite naturally — we omit the technical details here for brevity.

In (Ferragina et al., 2009) a comprehensive list of navigational operations supported by the index were introduced. Due to the lexicographical ordering of S, all children of an internal node occur at a specific range $[s,e]$ in S. For example, children of the root node in Figure 1(c) can be found on rows $[2,4]$. Operation $\mathsf{GetChild}(i)$ returns the range $[s,e]$ corresponding to all the children of $S[i]$ in $O(\log\sigma/\log\log n)$ time (we omit details here for brevity) (Ferragina et al., 2009). Similarly, $\mathsf{GetRankedChild}(i,j)$ returns the j-th child of i, which is simply $s+j-1$. The degree of node i is $\mathsf{GetDegree}(i) = e-s+1$ where $[s,e]$ is given by $\mathsf{GetChild}(i)$.

Computing Path Frequencies. Next we will give a recursive algorithm to output, for all unique root-originating paths, the number of times the path occurs, i.e. path's *frequency*, in each tree. For now, assume that we are given an index containing one tree T. At the start of the recursion, we initialize the current subpath P to be empty, and set $s = e = 1$. The following *invariant* holds throughout the recursion: at every step, the range $S[s,e]$ corresponds to all nodes having upward path equal to P.

Each recursion step proceeds as follows. First we enumerate all unique labels appearing on the range $S_\alpha[s,e]$ by using a range search on the Wavelet tree (cf. rows 1–2 in Figure 2). The labels can branch either to internal nodes or leaf nodes, or both. For each label c that branches with internal nodes, we locate

the first and last occurrence of c in $S_\alpha[s,e]$ (rows 8–9) and take their first and last child as the new range (rows 10-11). Then a recursive call is done for the new range $[s',e']$ and subpath $P' = cP$. However, if there are also leaf nodes branching with c, their frequencies must be passed on for the recursive call since leaves that match the path cP appear on $S[s,e]$ instead of the new interval (rows 5–7). Furthermore, remaining leaf symbols must be handled separately (rows 13–15). Finally, we output the frequency of the current subpath P, which equals the number of 1-bits in $S_{\mathsf{last}}[s,e]$ plus the leaf frequency passed on downwards in recursion (rows 16–17).

Let us give a short example using Figure 1(c). Assume that we arrive at the range $[5,7]$ which corresponds to subpath $P = \mathsf{BA}$. We branch with B which gives us the new range $[8,8]$. However, there is also a leaf branching with B in the range $[5,7]$ (and recall that we use lower-case to distinguish leaves), thus, when we recursively call for the new range $[8,8]$, we also pass on the information about the branching leaf. Final frequency of $P' = \mathsf{BBA}$ is then 2.

The time complexity of each recursion step is dominated by the range search on the Wavelet tree (rows 1–2), which requires (with a naive approach) time proportional to the length of the interval, i.e. $O((e-s+1)\log\sigma)$. Since the recursion iterates only over root-originating paths, the intervals $[s,e]$ are all non-overlapping. Thus, the total time complexity is $O(t\log\sigma)$. Moreover, we can generalize the frequency counting for a set of trees or multiple tree sets while retaining the same time complexity.

Computing the Kernel. We use a Dirac kernel to compare individual paths. The kernel is computed directly as a dot product between path feature vectors.

4 EXPERIMENTS

In this section, we evaluate the performance of path kernels against state-of-the-art graph kernels in a prediction task from (Saigo et al., 2010), where the EC number of a reaction is predicted. An EC code annotates the function of an enzymatic reaction in a four-level hierarchical numeric code "a.b.c.d", where the first level indicates the general class of the enzyme (ligases, lyases, isomerases, etc.) and following levels specify the reaction mechanisms. The fourth level is arbitrary index and ignored. Thus there are 270 full EC codes.

Reaction Dataset. We perform the experiments on a reaction set from KEGG LIGAND database representing common metabolic reactions (release 1.7.2010). A chemical reaction is a graph transformation, where substrates are transformed into products often catalyzed by an enzyme, which rearranges the bonds of the chemical compounds. We constructed graph representations of the reactions by modeling the substrates and products as two separate disjoint graphs with a bi-partite optimal atom mapping between the two graphs' nodes (see top of Figure 3) (Heinonen et al., 2011). A reaction graph is constructed by rerouting edges of the product side to the substrate side through the mapping, and removing product nodes (see bottom of Figure 3) (Felix et al., 2005).

The dataset consists of 15566 EC-labeled reaction graphs computed using optimal atom mappings. All reactions are theoretically capable of functioning in forward and backward directions, thus we include both versions by constructing a direction-invariant tensor kernel as in (Astikainen et al., 2011) resulting in 7783 reactions. Median size of reaction graphs is 38 and maximum 393.

Kernels for Reactions. We compare our path kernels to the simple walk kernel (up to length $k = 15$), shortest path kernel, and the RGK kernel by (Saigo et al., 2010), specifically introduced for reactions. In RGK an alternative reaction graph model is defined, which uses inner and outer marginal walk kernels to compare similarity of reactions.

The path index was implemented by reusing our own existing C/C++ implementations of Huffman-shaped Wavelet trees (Grossi et al., 2004) and bitvectors supporting rank and select queries (Jacobson, 1989). Optimal construction time and space are not yet achieved since our current implementation of the sorting phase requires $O(t\log^2 t)$ time and $\Theta(t\log t)$ bits of memory. We are currently planning to improve the sorting phase by plugging in a more sophisticated path sorting method (Ferragina et al., 2009). Table 1 gives a summary of the performance of the path index.

We ran the experiments with MMCRF hierarchical multilabel classification algorithm (Rousu et al., 2007). All kernels use $\lambda = 0.90$ and non-RGK kernels are tensor kernels. A 5-fold cross-validation procedure was used and an optimal C-parameter was chosen from $\{1, 10, 100, 1000, 10000\}$. We employ normalized quadratic kernels as they achieved consistently best results.

Results. The results are shown in table 2. A reaction mechanism is deemed correctly classified if the correct root-to-leaf branch of the EC hierachy is predicted by MMCRF. The walk kernel is clearly infe-

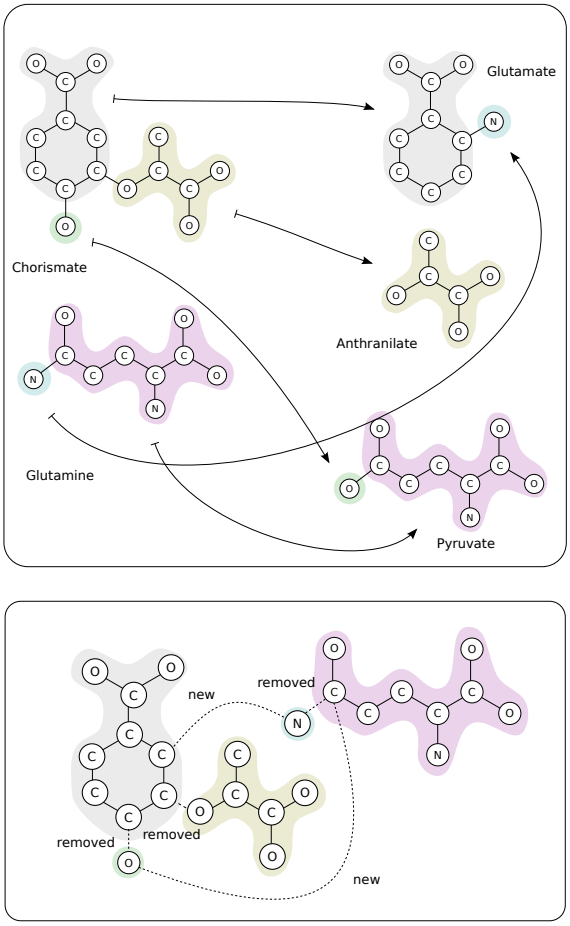

Figure 3: Reaction `R00986: Chorismate pyruvate-lyase` in forward direction and its optimal atom mapping (top). Atom mapping is highlighted with corresponding colors and the corresponding reaction graph is below. The "+1" edges are marked as new and "-1" edges are removed.

rior to the other kernels in this test. RGK and shortest paths kernels fared better achieving a test set error of 35.0% and 36.4%, respectively. Variants of the path kernels achieved a minimum of 24.3% test error.

We experimented with upper bounds 15 and 50 for path length. The results are similar or slightly better for the upper bound 15, indicating that most information resides in shorter paths. However the overfitting effect of the significantly larger feature space associated with the bound 50 is relatively small.

With compressed path index it is trivial to pick a subset of paths to focus on. We experimented with *core paths*, paths that go through modified edges (labeled "+1" or "-1"). These paths are most likely most relevant regarding the reaction transformation. The results show that using core paths decreases the error to 28.9% from 34.2% of the all path version. However, when using indicator feature values (all features are binary) the *all-path* kernel achieves the lowest error rates independent of the upper bound on the path length. It seems that core paths provides a clearer signal to the learning machine, but using indicators for all paths achieves an even stronger effect.

Table 1: Characteristics of the test data and performance results. Note that both construction time and space can still be optimized with a small engineering effort. Experiments run on Xeon X7350 CPU and 128 GB of memory.

# of reaction graphs	17,430
# of trees	746,438
# of tree nodes	279 mil.
# of tree leaves	91 mil.
max. tree depth	50
Index construction time	1.1 hours
Index construction space	4.4 GB
Final index size	1.1 GB
# of unique paths	21 mil.
Index frequency computation	176 s
Kernel computation (path length 50)	718 s
MMCRF run (average, 5-fold cv)	10 hours

Table 2: Prediction of full EC class. Core path kernel only includes paths with "+1" or "-1" edges, while indicator kernels contain only binary values.

Kernel	k	Tr. error (%)	Ts. error (%)
Walk	15	52.9	61.1
RGK	inf	27.8	35.0
Shortest paths		21.5	36.4
Core paths	50	14.9	28.9
Core paths, ind	50	14.5	27.8
All paths	50	19.6	34.2
All paths, ind	50	9.1	25.6
Core paths	15	15.0	28.3
Core paths, ind	15	14.7	27.3
All paths	15	20.0	33.7
All paths, ind	15	9.2	**24.3**

An experiment with the max kernel had a small less than 1% positive effect on accuracies (data not shown). The max kernel is not positive semi-definite, although the smallest negative eigenvalue is relatively small. The MMCRF seemed to converge in spite of the indefinite setting. The values on Table 2 are from the max kernel.

Figure 4 shows the performance of five main kernels on the EC main class only. The main classes are most general and are thus most difficult to predict. Here, RGK kernel is on par with path kernels. The first EC class of oxidoreductases is most difficult to predict. The high performance on the sixth class of ligases can be explained by the homogeneity of the ligases.

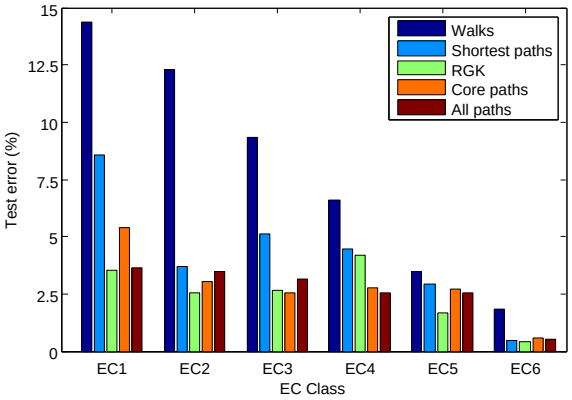

Figure 4: Prediction results for the six main EC classes. The first EC class (oxidoreductases) is most difficult, while the last (ligases) is well predicted with any method.

5 DISCUSSION AND CONCLUSIONS

The path index can also be used for *on-line* path frequency queries: given any path P of length $m \leq h$, where h is the maximum path length enumerated, we can output the frequency of the path P in all graphs in just $O(m \log \sigma + \mathsf{output})$ time, where output is the size of the output, i.e. the number of distinct graphs having frequency that is greater than zero. Details are out of the scope of this paper, but this type of on-line *feature query* might be interesting when computing kernels in iterative manner. Another interesting direction would be to implement feature selection or ℓ_1 regularized learning methods for graph data making use of the efficient access to features.

We presented a method for efficiently computing all-paths kernels for graph data. Our approach relies on computing and storing a single compressed path index of all graphs, which can subsequently be efficiently queried for the purposes for graph kernel or feature vector computation. We demonstrate the computational feasibility of the approach by computing a path index for graph representations of KEGG reactions. Our experiments show that path kernels give significant improvements over walk kernels in the reaction mechanism prediction task.

ACKNOWLEDGEMENTS

We are grateful to Petteri Kaski, Mikko Koivisto and Craig Saunders for insightful discussions. This work was funded by the Academy of Finland grants 1140727 and 118653, the Graduate School Hecse and by the PASCAL2 (IST grant-2007-216886).

REFERENCES

Astikainen, K., Holm, L., Pitkänen, E., Szedmak, S., and Rousu, J. (2011). Structured output prediction of novel enzyme function with reaction kernels. In *Biomedical Engineering Systems and Technologies*, pages 367–378. Springer.

Borgwardt, K., Ong, C., Schönauer, S., Vishwanathan, S., Smola, A., and Kriegel, H.-P. (2005). Protein function prediction via graph kernels. *Bioinformatics*, 21:i47.

Demco, A. (2009). *Graph Kernel Extension and Experiments with Application to Molecule Classification, Lead Hopping and Multiple Targets*. PhD thesis, University of Southampton.

Felix, H., Rossello, F., and Valiente, G. (2005). Optimal artificial chemistries and metabolic pathways. In *Proc. 6th Mexican Int. Conf. Computer Science*, pages 298–305. IEEE Computer Science Press.

Ferragina, P., Luccio, F., Manzini, G., and Muthukrishnan, S. (2009). Compressing and indexing labeled trees, with applications. *J. ACM*, 57:4:1–4:33.

Ferragina, P., Manzini, G., Mäkinen, V., and Navarro, G. (2007). Compressed representations of sequences and full-text indexes. *ACM Transactions on Algorithms (TALG)*, 3(2):article 20.

Gärtner, T. (2003). A survey of kernels for structured data. *ACM SIGKDD Explorations Newsletter*, 5:49–58.

Grossi, R., Gupta, A., and Vitter, J. S. (2004). When indexing equals compression: experiments with compressing suffix arrays and applications. In *Proc. 15th annual ACM-SIAM Symposium on Discrete Algorithms*, pages 636–645, Philadelphia, PA, USA. SIAM.

Heinonen, M., Lappalainen, S., Mielikäinen, T., and Rousu, J. (2011). Computing atom mappings for biochemical reactions without subgraph isomorphism. *J. Comp. Biology*, 18:43–58.

Jacobson, G. (1989). *Succinct Static Data Structures*. PhD thesis, Carnegie–Mellon. CMU-CS-89-112.

Kashima, H., Tsuda, K., and Inokuchi, A. (2003). Marginalized kernels between labeled graphs. In *Proc. 20th Int. Conf. on Machine Learning (ICML)*, pages 321–328.

Mahe, P., Ueda, N., Akutsu, T., Perret, J.-L., and Vert, J.-P. (2005). Graph kernels for molecular structure-activity relationship analysis with support vector machines. *J. Chem. Inf. Model.*, 45:939–951.

Ralaivola, L., Swamidass, S., Saigo, H., and Baldi, P. (2005). Graph kernels for chemical informatics. *Neural Networks*, 18:1093–1110.

Rousu, J., Saunders, C., Szedmak, S., and Shawe-Taylor, J. (2007). Efficient algorithms for max-margin structured classification. *Predicting Structured Data*, pages 105–129.

Saigo, H., Hattori, M., Kashima, H., and Tsuda, K. (2010). Reaction graph kernels predict ec numbers of unknown enzymatic reactions in plant secondary metabolism. *BMC Bioinformatics*, 11:S31.

Shawe-Taylor, J. and Christianini, N. (2004). *Kernel Methods for Pattern Analysis*. Cambridge University Press.